QUARTERLY JOURNAL OF THE ROYAL METEOROLOGICAL SOCIETY
Q. J. R. Meteorol. Soc. **00**: 1–**??** (0000)
Published online in Wiley InterScience
(www.interscience.wiley.com) DOI: 10.1002/qj.000

Spectrum of infrasound radiation from supercell storms

M. Akhalkatsi[a], G. Gogoberidze[a∗]
Institute of theoretical physics, Ilia State University, 2a Kazbegi ave., 0160 Tbilisi, Georgia

Abstract:
We consider the generation of acoustic waves by turbulent convection and perform spectral analysis of a monopole source of sound related to the heat production by condensation of moisture. A quantitative explanation of the correlation between intensity of infrasound generated by supercell storms and later tornado formation is given. It is shown that low lifting condensation level (LCL) and high values of convective available potential energy (CAPE), which are known to favor significant tornadoes, also lead to a strong enhancement of supercells low frequency acoustic radiation.

KEY WORDS convection, supercell storms, tornados, infrasound.

Received ; Revised ; Accepted

1 Introduction

Recent observations of infrasound originating from regions of severe weather show that infrasound dominant frequency occurs in a passband from 0,5 to 2,5 Hz, with peak frequencies between 0,5 and 1 Hz (e.g. Bedard, 2005; Bedard *et al*., 2004a). Analyzing acoustic radiation from severe thunderstorms, Bedard (2004a) concluded that radiation of infrasound in this passband is not a natural consequence of all severe weather. Infrasound of a tornadic thunderstorm is much stronger than infrasound of a nonsevere weather system and therefore, mesocyclones or tornadoes may be a primary mechanism for infrasound production in this frequency range (Szoke *et al*., 2004).

Detection of infrasound appears to have significant potential for improving tornado forecasting. The acoustic power radiated by strong convective storm system could be as high as 10^7 watts (Georges, 1988) and infrasound below 1 Hz can travel for distances of thousands of kilometers from a source without significant absorption.

Over the years, several potential sound generation mechanisms were compared with measured characteristics of infrasound (Georges and Greene, 1975; Georges, 1988; Bedard and Georges, 2000; Beasley *et al*., 1976). Such mechanisms include release of latent heat, dipole radiators, boundary layer turbulence, lightning, electrostatic sources and vortex sound (radial vibrations and the co-rotation of suction vortices). Georges (1976) eliminated many sources as likely candidates and concluded that vortex sound was the most likely model. Bedard (2005) also found that the radial vibration model (Abdullah, 1966) is most consistent with infrasonic data. This model predicts that the fundamental frequency of radial

∗Correspondence to: E-mail: gogober@geo.net.ge

vibration will be inversely proportional to core radius. A radius of about 200 m will produce a frequency of 1 Hz. Schecter *et al*. (2008) performed numerical simulation of the adiabatic generation of infrasound by tornadoes and also simulated the infrasound radiated from a single-cell non-tornadic thunderstorm in a shear-free environment, using Regional Atmospheric Modeling System (RAMS). In the latter simulation dominant infrasound in the $0.1 - 10$ Hz frequency band, so called ”thunderstorm noise” appeared to radiate from the vicinity of the melting level, where diabatic processes involving hail were active. They found that 3D Rossby waves of a tornado-like vortices can generate stronger $0.1 - 10$ Hz infrasound at or above the simulated non-tornadic thunderstorm noise if maximum wind speed of the vortex exceeds a modest threshold.

Georges and Green (1975) noted that infrasound often precedes an observed tornado by up to an hour. Many other case studies of infrasound associated with tornadoes and tornadic storms (Bedard *et al*., 2004a; Bedard *et al*., 2004b) are consistent with this result. Bedard *et al*. (2004b) analyzed all significant infrasonic signals data collected in 2003 during the continuous Infrasonic Network (ISNeT) operation. Summarizing differences between predicted acoustic signal arrival times from reported tornados and start times of infrasonic detection they concluded that infrasound is usually produced substantially before (0.5 - 1 hrs) reports of tornadoes and that there could be other sound generation processes active not related to tornadic vortices. Bedard *et al*. (2004b) also indicated the difference between the infrasonic bearing sectors and the vortex location and concluded that, although the storm environment wind and temperature gradient could be responsible for bearing deviations, there remains the possibility that another storm feature could radiate infrasound from another location within the storm (bedard, 2004).

Broad and smooth spectra of observed infrasound radiation indicates that turbulence is a promising sources of the radiation. Acoustic radiation from turbulent convection was studied by Akhalkatsi and Gogoberidze (2009) taking into account effects of stratification, temperature fluctuations and moisture of air, using Lighthill’s acoustic analogy. It was shown for typical parameters of strong convective storms, infrasound radiation should be dominated by a monopole acoustic source related to the moisture of the air. The total power of this source is two orders higher than thermo-acoustic and Lighthill’s quadrupole radiation power, being of order 10^7 watts, in qualitative agreement with observations of strong convective storms (Bowman and Bedard, 1971; Bedard and Georges, 2000; Georges and Greene, 1975; Georges, 1973).

This paper represents an extension of the study performed by Akhalkatsi and Gogoberidze (2009). Namely, we extended earlier study in two directions. Firstly, we perform detailed spectral analysis of a monopole source related to heat production during the condensation of moisture. Assuming homogeneous and stationary turbulence we calculate the spectrum of acoustic radiation. Secondly, we perform detailed analysis of the sound generated by a monopole source as well as infrasound observations and present a qualitative explanation of the observed high correlation between intensity of low frequency infrasound signals from supercell storms and the probability of later tornado formation. We show that acoustic power of a monopole source related to the moisture of the air strongly depends on the same parameters that are the most promising in discriminating between nontornadic and tornadic supercells according to the recent study of tornadogenesis (Markowsky and Richardson, 2008). In particular, low

Prepared using *qjrms3.cls*
DOI: 10.1002/qj

lifting condensation level (LCL) is known to favor significant tornadoes (Rasmussen and Blanchard, 1998; Thompson *et al*., 2003). On the other hand, low LCL height means that air in the updraft is saturated at lower heights and consequently has a higher temperature at the level of saturation. We show that the increase of temperature causes rapid enhancement of monopole acoustic power related to heat production during condensation of moisture.

Another widely used supercell and tornado forecasting parameter is supercell environmental convective available potential energy (CAPE). It is known that high values of CAPE (especially, occurring closer to the surface) assist tornado formation (Weisman and Klemp, 1982; Rotunno and Klemp, 1982; Rasmussen, 2003; Rasmussen and Blanchard, 1998; Thompson *et al*., 2003). Furthermore, high values of CAPE means high updraft velocity and therefore the increased rms of turbulent velocities, which results in a strong enhancement of total acoustic power.

The paper is organized as follows: General formalism is presented in section 2. Spectral analysis of acoustic radiation is performed in section 3. Correlation between intensity of infrasound radiation by supercell storm and probability of tornado formation is discussed in section 4. Conclusions are given in section 5.

2 General formalism

The dynamics of convective motion of moist air is governed by the continuity, Euler, heat, humidity and ideal gas state equations:

$$\frac{D\rho}{Dt} + \rho\nabla\cdot\mathbf{v} = 0, \tag{1}$$

$$\rho\frac{D\mathbf{v}}{Dt} = -\nabla p - \rho\nabla\Phi, \tag{2}$$

$$T\frac{Ds}{Dt} = -L_\nu\frac{Dq}{Dt}, \tag{3}$$

$$\rho = \frac{p}{RT}\frac{1}{1-q+q/\epsilon} = \frac{p}{RT}\frac{1}{1+aq}, \tag{4}$$

where $\mathbf{v}$, ρ and p are velocity, density and pressure, respectively; $D/Dt \equiv \partial/\partial t + \mathbf{v}\cdot\nabla$ is Lagrangian time derivative; L_ν is the latent heat of condensation and q is the humidity mixing ratio

$$q \equiv \frac{\rho_\nu}{\rho}. \tag{5}$$

Here ρ_ν is the mass of water vapor in a unit volume; Φ is gravitational potential energy per unit mass and $\nabla\Phi \equiv -\mathbf{g}$. $\epsilon \equiv m_\nu/m_d \approx 0.622$ is the ratio of molecular masses of water and air; $a = 0.608$ and R is the universal gas constant.

In the set of Eqs. (1)-(4) diffusion and viscosity effects are neglected due to the fact that they have a negligible influence on low frequency acoustic wave generation and propagation.

Using the standard procedure of Lighthill's acoustic analogy (Goldstein 2002), manipulation of Eqs. (1)-(4) yield the equation governing sound generation by turbulence for a moist atmosphere in terms of the total enthalpy (Akhalkatsi and Gogoberidze, 2009)

$$\left(\frac{D}{Dt}\left(\frac{1}{c_s^2}\frac{D}{Dt}\right) - \frac{\nabla p\cdot\nabla}{\rho c_s^2} - \nabla^2\right)B = S_L + S_T + S_q + S_m + S_\gamma, \tag{6}$$

where $\gamma \equiv c_p/c_v$ is the ratio of specific heats,

$$c_s \equiv \left(\frac{\partial p}{\partial \rho}\right)^{1/2}_{s,q} \tag{7}$$

DOI: 10.1002/qj
Prepared using qjrms3.cls

is the sound velocity and enthalpy B is determined by the generalized Bernoulli theorem

$$B \equiv E + \frac{p}{\rho} + \frac{v^2}{2} + \Phi, \tag{8}$$

where E is internal energy. B is constant in the steady irrotational flow and at large distances from acoustic sources perturbations of B represent acoustic waves (Howe, 2001).

The terms on the right hand side of Eq. (6) represent acoustic sources:

$$S_L \equiv \left(\nabla + \frac{\nabla p}{\rho c_s^2} \right) \cdot (\omega \times \mathbf{v}), \tag{9}$$

$$S_T \equiv - \left(\nabla + \frac{\nabla p}{\rho c_s^2} \right) \cdot (T \nabla s), \tag{10}$$

$$S_q \equiv \frac{\partial}{\partial t} \left(\frac{\gamma T}{c_s^2} \frac{Ds}{Dt} \right) + (\mathbf{v} \cdot \nabla) \left(\frac{T}{c_s^2} \frac{Ds}{Dt} \right), \tag{11}$$

$$S_m \equiv \frac{\partial}{\partial t} \left(\frac{a}{1 + aq} \frac{Dq}{Dt} \right), \tag{12}$$

$$S_\gamma \equiv p \frac{\partial \gamma}{\partial q} \left(\frac{\partial q}{\partial t} (\mathbf{v} \nabla) p - \frac{\partial p}{\partial t} (\mathbf{v} \nabla) q \right). \tag{13}$$

To make further mathematical analysis more tractable we will make standard simplifying assumptions: for low Mach number flow all convective derivatives in Eq. (6) can be replaced by time derivatives $\partial / \partial t$ (Goldstein, 1976); for the acoustic pressure in far field we can use

$$p'(\mathbf{x}, t) \approx \rho_0 B(\mathbf{x}, t); \tag{14}$$

we neglect nonlinear effects of acoustic wave propagation and scattering of sound by vorticity; we also neglect the influence of stratification on the acoustic wave generation process and consider background thermodynamic parameters in Eq. (6) as constants. The later assumption is valid if the wavelength of generated acoustic waves do not exceed the stratification length scale (Stein, 1967),

$$\lambda \lesssim H \equiv \frac{c_s^2}{g} \approx 10^4 \mathrm{m}. \tag{15}$$

With these assumptions Eq. (6) reduces to

$$\frac{1}{\rho_0} \left(\frac{1}{c_s^2} \frac{\partial^2}{\partial t^2} - \nabla^2 \right) p' = S_L + S_T + S_\gamma + S_q + S_m \tag{16}$$

with

$$S_L \approx \nabla \cdot (\omega \times \mathbf{v}), \tag{17}$$

$$S_T \approx - \nabla \cdot (T \nabla s), \tag{18}$$

$$S_\gamma = p \frac{\partial \gamma}{\partial q} \left(\frac{\partial q}{\partial t} (\mathbf{v} \nabla) p - \frac{\partial p}{\partial t} (\mathbf{v} \nabla) q \right). \tag{19}$$

$$S_m \approx \frac{a}{1 + aq} \frac{\partial^2 q}{\partial t^2}, \tag{20}$$

$$S_q \approx - \frac{\gamma L_\nu}{c_s^2} \frac{\partial^2 q}{\partial t^2}, \tag{21}$$

First three terms on the right hand side of Eq. (16) represent well known sources of sound: the first term represents Lighthill's quadrupole source (Lighthill, 1952); the second term is a dipole source related to temperature fluctuations (Goldstein, 1976); S_γ is a monopole source related to variability of adiabatic index and usually has negligible acoustic output (Howe, 2001). As it was shown in Akhalkatsi and Gogoberidze (2009), in the case of saturated moist air turbulence there exists two additional monopole sources of sound, S_q and S_m, related to non-stationary heat and mass production during condensation of moisture, respectively.

S_q and S_m produce monopole radiation and physically have the following nature: suppose there exist two saturated air parcels of unit mass with different temperatures T_1 and T_2 and water masses $m_\nu(T_1)$ and $m_\nu(T_2)$. Mixing of these parcels leads to the condensation of water

Prepared using qjrms3.cls
DOI: 10.1002/qj

due to the fact that

$$2m_\nu(T_1/2+T_2/2) < m_\nu(T_1)+m_\nu(T_2). \tag{22}$$

Condensation of water leads to two effects important for sound generation: production of heat and decrease of gas mass. Both of these effects are known to produce monopole radiation (Goldstein, 1976; Howe, 2001). Consequently, turbulent mixing of saturated air with different temperatures will lead not only to dipole thermo-acoustical radiation, but also to monopole radiation.

As it was shown by Akhalkatsi and Gogoberidze (2009), for typical parameters of supercell storms acoustic radiation is dominated by a monopole source related to the heat production S_q. The total acoustic power can be estimated as

$$N_q \sim \frac{\rho_0\gamma^2 L_\nu^2 \Delta q^2 M_t^4}{l c_s} F_1, \tag{23}$$

where Δq is the rms of humidity mixing ratio perturbations; l is the length scale of energy containing turbulent eddies; $M_t \equiv v/c_s \ll 1$ is turbulent Mach number and F_1 is the volume occupied by saturated moist air turbulence. For typical parameters S_q is much greater, than other sources of sound and two orders of magnitude stronger then Lighthill's quadrupole source.

3 Spectral Decomposition

In this section we study the spectrum of acoustic radiation related to S_q. Dropping all other source terms (16) reduces to the inhomogeneous wave equation

$$\frac{1}{\rho_0}\left(\frac{1}{c_s^2}\frac{\partial^2}{\partial t^2} - \nabla^2\right) p' = S_q. \tag{24}$$

Using standard methods for spectral analysis of the inhomogeneous wave equation (Goldstein, 1976; Howe, 2001; Gogoberidze *et al.*, 2007), after a long but straightforward calculation, for the spectrum of temperature fluctuations $I(\mathbf{x},\omega)$ we obtain

$$I(\mathbf{x},\omega) = \frac{\omega^4\pi\rho_0\gamma^2L_\nu^2}{2c_s^5|\mathbf{x}|^2}\left(\frac{\partial^2 q_s}{\partial T^2}\right)^2 \int \mathrm{d}^3\mathbf{x}' H\left(\mathbf{x}', \frac{\mathbf{x}}{|\mathbf{x}|}\omega, \omega\right), \tag{25}$$

where $H(\mathbf{x}',\mathbf{k},\omega)$ is a spectral tensor of temperature fluctuations and represents a Fourier transform of a two point time delayed forth order correlation function of temperature fluctuation.

Equation (25) allows to calculate the spectrum of sound radiated by a monopole source related to the moisture, if statistical properties of the turbulent source can be determined. For our calculations we consider the Von Karman model of stationary and homogeneous turbulence, which is given by (Hinze, 1975)

$$E_k = C_K \varepsilon^{2/3} k_0^{-5/3} \frac{(k/k_0)^4}{[1+(k/k_0)^2]^{17/6}}. \tag{26}$$

for $k < k_d$ and $E_k = 0$ for $k > k_d$, where $2\pi/k_d$ is the dissipation length scale.

The Von Karman spectrum reduces to the Kolmogorov spectrum in the inertial interval ($k \gtrsim k_0$), but also satisfactorily describes the energy spectrum in the energy containing interval, which is a dominant contributor to acoustic radiation.

As is known (Monin and Yaglom, 1975), temperature fluctuations of homogeneous isotropic and stationary turbulence behaves like a passive scalar and therefore has the same spectrum as velocity fluctuation. Therefore for the spectral function of temperature fluctuation $F(\mathbf{k},\tau)$, which is spatial Fourier transform of temperature correlation function $\Theta(\mathbf{r},\mathbf{t}) = \langle \mathbf{T}'(\mathbf{x}+\mathbf{r},\mathbf{t})\mathbf{T}'(\mathbf{x},\mathbf{t})\rangle$, we assume

$$F(\mathbf{k},\tau) = \frac{Q_k}{4\pi k^2} f(\eta_k,\tau), \tag{27}$$

DOI: 10.1002/qj

where

$$Q_k = \Delta T^2 k_0^{-1} \frac{(k/k_0)^4}{[1+(k/k_0)^2]^{17/6}}. \tag{28}$$

In equation Eq. (27) $\triangle T$ is rms of the temperature fluctuation, η_k is the autocorrelation function defined as

$$\eta_k = \sqrt{\frac{k^3 E_k}{2\pi}} \tag{29}$$

and $f(\eta_k, \tau)$ characterizes the temporal decorrelation of turbulent fluctuations, such that it becomes negligibly small for $\tau \gg 1/\eta_k$.

For $f(\eta_k, \tau)$ we use a square exponential time dependence (Kraichnan, 1964)

$$f(\eta_k, \tau) = \exp\left(-\frac{\pi}{4}\eta_k^2 \tau^2\right). \tag{30}$$

For a homogeneous turbulence two point time delayed forth order correlation function of temperature fluctuations $R(\mathbf{x}', \mathbf{x}' + \mathbf{r}, \tau)$ is related to the temperature correlation function by means of the following relation (Monin and Yaglom, 1975)

$$R(\mathbf{x}', \mathbf{x}' + \mathbf{r}, \tau) = 2\left\langle T'(\mathbf{r}, \tau) T'(\mathbf{r}, \tau)\right\rangle \left\langle T'(\mathbf{r}, \tau) T'(\mathbf{r}, \tau)\right\rangle. \tag{31}$$

Using Eqs. (27),(29),(30) and the convolution theorem we find

$$H(\mathbf{k}, \omega) = 2\int \mathrm{d}\mathbf{k}_1^3 \mathrm{d}\omega_1 g(\mathbf{k}_1, \omega_1) g(\mathbf{k} - \mathbf{k}_1, \omega - \omega_1), \tag{32}$$

where

$$g(\mathbf{k}, \omega) = \frac{Q_k}{4\pi^2 \eta_k} \exp\left(-\frac{\omega^2}{\pi \eta_k^2 k^2}\right). \tag{33}$$

For low Much number turbulence one can use the so called aeroacoustic approximation (Goldstein, 1976), which for the Fourier spectrum implies that in Eq. (25) instead of $H(\mathbf{x}', \omega\mathbf{x}/|\mathbf{x}|, \omega)$ one can set $H(\mathbf{x}', 0, \omega)$.

Performing the integration with respect to frequency in Eq. (32) as well as angular variables in wave number space we obtain

$$H(0, \omega) = \frac{\sqrt{2}}{4\pi^2}\int_{k_0}^{k_d} \mathrm{d}k \frac{Q_k^2}{k^2 \eta_k} \exp\left(-\frac{\omega^2}{2\pi \eta_k^2}\right). \tag{34}$$

The aeroacoustic approximation simplifies finding asymptotic limits for the spectrum. In the low-frequency regime, taking the limit $\omega \to 0$ we obtain

$$H(0, \omega) \sim \frac{1}{10\pi^{3/2}} \frac{\Delta T^4}{k_0^4 M c_s}. \tag{35}$$

For the spectrum this means $I(\mathbf{x}, \omega) \backsim \omega^4$. Physically, these frequencies are lower than the lowest characteristic frequency in the problem, corresponding to the eddy turnover time on the energy containing scale.

At high frequencies $\omega \gg k_0 M R^{1/2}$, the integral in Eq. (34) is dominated by the contribution from its upper limit and we get

$$H(0, \omega) \sim \frac{3}{8\pi^{3/2}} \frac{\Delta T^4}{k_0^2} \frac{M c_s}{\omega^2} \exp\left(-\frac{\omega^2}{k_0^2 M^2 c_s^2 R}\right) \tag{36}$$

and

$$I(\mathbf{x}, \omega) \sim \omega^2 \exp\left(-\frac{\omega^2}{k_0^2 M^2 c_s^2 R}\right). \tag{37}$$

The functional form of the high-frequency suppression is determined by the specific form of the time autocorrelation function of turbulence Eq. (30) (Kraichnan, 1964), but for any autocorrelation the amplitude of emitted waves should be very small in this band. Physically, this limit corresponds to radiation frequencies which are larger than any frequencies of turbulent motions; consequently, no scale of turbulent fluctuations generates these radiation frequencies directly, and the resulting small radiation amplitude is due to the sum of small contributions from many lower-frequency source modes. Since the integral

DOI: 10.1002/qj

is dominated by the upper integration limit, the highest-frequency source fluctuations (which contain very little of the total turbulent energy) contribute most to this high-frequency radiation tail.

In the intermediate frequency regime, $k_0 M c_s < \omega < k_0 M c_s R^{1/2}$, the integral in Eq. (34) is dominated by the contribution around k_1, where $\eta_{k_1} \approx \omega$. The width of the dominant interval is $\Delta k_1 \sim k_1$. Physically, this implies that radiation emission at some frequency in this range is dominated by turbulent vortices of the same frequency. Consequently, for the inertial interval we obtain following estimate

$$H(0,\omega) \simeq \frac{1}{3\pi^{3/2}} \frac{\Delta T^4}{k_0^4 M c_s} \left(\frac{k_0 M c_s}{\omega} \right)^{15/2} \qquad (38)$$

and

$$I(\mathbf{x},\omega) \sim \omega^{-7/2}. \qquad (39)$$

We performed numerical integration of Eq. (34) for the Von Karman model of turbulence and determined normalized spectrum of acoustic radiation to be

$$I_N(\nu) = \frac{4\sqrt{2}\pi c_s^2 |\mathbf{x}|^2}{\rho_0 \gamma^2 L_\nu^2 k_0 v_0^4 \Delta T^4 F_1} I(\mathbf{x},\omega). \qquad (40)$$

The normalized spectrum for characteristic length scale of energy containing eddies $l = 2\pi/k_0 = 15$ m and characteristic rms velocity $v_0 = 5$ m s^{-1} is presented in Fig. 1. As can be seen for these typical parameters the peak frequency of infrasound radiation is $\nu_{peak} \approx 0.8$ Hz.

As shown by Akhalkatsi and Gogoberidze (2009), the peak frequency of acoustic radiation is inversely proportional to the turnover time of energy containing turbulent eddies $\nu_{peak} \sim v_0/l$, whereas total acoustic power is proportional to v_0^4, ΔT^4 and inversely proportional to l.

4 Infrasound correlation with tornadoes

Severe storm forecasting operations are based on several large scale environmental, storm scale, meso-beta scale kinematic and thermodynamic parameters (Davies-Jones, 1993; Lemon and Doswell, 1979; Markowski *et al*., 1998, Markowski *et al*., 2002), used to study the potential of severe weather, thunderstorm structure and organization to produce tornadoes. Recent climatological studies of thunderstorms using real-time radar data combined with observations of near-storm environment have been focused on the utility of various supercell and tornado forecast parameters (CAPE, Storm Relative Helicity - SRH, Bulk Richardson number - BRN and other parameters). Two parameters have been established to be the most promising in discriminating between nontornadic and tornadic supercells: boundary layer water vapor concentration (LCL hight) and low level vertical wind shear (Markowski and Richardson, 2008; Rasmussen, 2003; Thompson and Edwards, 2000).

Examining a baseline climatology of parameters commonly used in supercell thunderstorm forecasting and research, Rasmussen and Blanchard (1998) established that the parameter that shows the most utility for discriminating between soundings of supercells with significant tornadoes and supercells without significant tornadoes is LCL height. The height of the LCL appeared to be generally lower for supercells with significant tornadoes than those without. Rasmussen and Blanchard (1998) also found that for storms producing large (at least 5-cm wide) hail only, without at least F2 strength tornadoes, the LCL heights were significantly higher than for ordinary thunderstorms. In their study half of the tornadic supercells soundings had LCLs below 800 m, while LCL heights above about 1200 m were associated with decreasing likelihood of significant tornadoes. They concluded

Q. J. R. Meteorol. Soc. **00**: 1–**??** (0000)
DOI: 10.1002/qj

that stronger evaporational cooling of moist downdraft leads to greater outflow dominance of storms in high LCL settings and low heights increase the likelihood of supercells being tornadic.

The work of Thompson and Edwards (2000) on assessing utility of various supercell and tornado forecasting parameters supports the finding that supercells above deeply mixed convective boundary layers, with relatively large dew point depressions and high LCL, often do not produce tornadoes even in environments of large CAPE and/or vertical shear. They found the LCL to be markedly lower for supercells producing significant tornadoes than for those producing weak tornadoes, which were in turn lower than for nontornadic supercells. Particularly, no strong and violent tornadoes occurred for supercells with LCL > 1500 m.

Studying the relationship between Rear flank downdraft (RFD) thermodynamic characteristics and tornado likelihood Markowski *et al*. (2002) found that low LCL favors formation of significant tornadoes because the boundary layer relative humidity somehow alters the RFD and outflow character of supercells. Relatively warm and buoyant RFDs, which are supposed to be necessary for the genesis of significant tornadoes, were more likely in moist low-level environments than in dry low-level environments (Markowski *et al*. 2002). It appeared that relatively dry boundary layers, characterized by higher LCLs, support more low-level cooling through the evaporation of rain, leading to stronger outflow, which could have been decreasing the likelihood of significant tornadoes in supercells. These are possible explanations for finding that the LCL height is generally lower in soundings associated with tornadic suppercells versus nontornadic (Rasmussen and Blanchard, 1998; Thompson and Edwards, 2000).

Thompson *et al*. (2003) reinforced the findings of previous studies related to LCL height as an important discriminator between significantly tornadic and nontornadic supercells and concluded that the differences in LCL heights across all storm groups studied were statistically significant, though the differences appeared to be operationally useful only when comparing significantly tornadic and nontornadic supercells. The lower LCL heights of the significantly tornadic storms supported the hypothesis of Markowski *et al*. (2002) that increased low-level relative humidity (RH) may contribute to increased buoyancy in the rear flank downdraft and an increased probability of tornadoes.

In idealized numerical simulations Markowski *et al*. (2003) investigated the effects of ambient LCL and the precipitation character of a rain curtain on the thermodynamic properties of downdraft, and ultimately on tornado intensity and longevity. The simulations were consistent with the observation that high boundary layer relative humidity values (i.e., low LCL height and small surface dewpoint depression) are associated with relatively warmer RFDs and more significant tornadogenesis than environments of relatively low boundary layer relative humidity.

These findings of low LCL favoring significant tornadoes could explain observed high correlation between low frequency infrasound signals from supercell storm and later tornado formation.

Acoustic power of a monopole source related to the heat production during condensation of moisture can been estimated as (Akhalkatsi and Gogoberidze, 2009):

$$N_q \sim \frac{\rho_0}{lc_s}[\gamma L_\nu]^2\left[\frac{M_t\Delta T}{T}\right]^4 f^2(T_c)F_1, \qquad (41)$$

DOI: 10.1002/qj

where

$$f(T_c) \approx 6.8 \cdot 10^4 \frac{273.15 + T_c}{(243.5 + T_c)^4} \exp\left(\frac{17.67 T_c}{T_c + 243.5}\right). \tag{42}$$

and $T_c = T - 273.15$ is the temperature in degree Celsius.

Due to the numerator in the exponent, $f(T_c)$ strongly depends on temperature, e.g., $f(T_C = 10°)/f(T_C = 0°) \approx 2$ and according to multiplier $f^2(T_c)$ in Eq. (41), increase of saturated air temperature causes rapid enhancement of total acoustic power radiated by a monopole source.

On the other hand, low LCL height means low level air in the updraft motion being saturated and consequently, higher temperature of saturated moist air. Therefore, the lower LCL heights contribute to increased total acoustic power radiated by a monopole source related to the heat production during the condensation of moisture. As a result, enhanced low frequency infrasound signals from supercell storm appear to be in strong correlation with an increased probability of tornadoes.

It is also known (Weisman and Klemp, 1982; Rotunno and Klemp, 1982; Rasmussen, 2003; Rasmussen and Blanchard, 1998; Thompson *et al*., 2003)that high values of supercell CAPE assist tornado formation. Indeed, high values of CAPE lead to an increase of the updraft persistence and thunderstorm activity and therefore increase probability of tornado formation. According to recent studies relatively larger CAPE occurs closer to the surface, which could produce more intense low-level stretching of vertical vorticity required for low-level mesocyclone intensification and perhaps tornadogenesis (Rasmussen, 2003, McCaul, 1991; McCaul and Weisman, 1996) is associated with low LCLs. Rasmussen (2003) found the 03-km above ground level (AGL) CAPE to be possibly important in discriminating between environments supportive of significant tornadoes and those that are not.

High values of CAPE mean high updraft velocity caused by large low-level accelerations and increased rms of turbulent velocities. According to Eq. (41) $N_q \sim M_t^4$, Therefore increasing rms of turbulent velocities results in strong enhancement of total acoustic power.

5 Conclusions

In this paper we have performed detailed spectral analysis of a monopole source of sound related to heat production during condensation of moisture, which is supposed to be dominant in the infrasound radiation observed from strong convective storms. We have also discussed the relationship between the acoustic power of this source and certain significant tornado forecast parameters. Particularly, low LCL, which is known to favor significant tornadoes (Rasmussen and Blanchard, 1998; Thompson *et al*., 2003) implying warmer air at the level of saturation. We have shown that the increase of temperature causes rapid enhancement of acoustic power. High values of CAPE (especially, occurring closer to the surface), which assist tornado formation (Weisman and Klemp, 1982; Rotunno and Klemp, 1982; Rasmussen, 2003; Rasmussen and Blanchard, 1998; Thompson *et al.*, 2003), means high updraft velocity and therefore, increased rms of turbulent velocities, which results in strong enhancement of total acoustic power.

ISNeT data combined with the information from Doppler Radar may help to improve tornado forecast and reduce false alarms from non-tornadic supercells. Recent studies comparing ISNeT output with occurrences of tornadoes (Bedard *et al.*, 2004a) and correlating ISNeT signals with detailed radar output (Szoke *et al*., 2004) show, that infrasound of a tornadic thunderstorm is much

DOI: 10.1002/qj

stronger than the infrasound of a nonsevere weather system. Correlation between the intensity of infrasound signals and probability of later tornado formation indicates the potential for discriminating between supercells that produce tornadoes and those that do not. Therefore, information from an infrasound detecting system may help to determine potentially tornadic storms.

Acknowledgements

G. G. acknowledges partial support from Georgian NSF ST06/4-096 and 07/406/4-300 grants.

References

Abdullah A. J. 1966. The "musical" sound emitted by a tornado. *Mon. Wea. Rev.*, 94, 213220

Akhalkatsi M. and Gogoberidze G. 2009. Infrasound generation by tornadic supercell storms. *Quart. J. Roy. Meteor. Soc.*, 135, 641, 935-940

Beasley W.H., Georges T.M. and Evans M.W. 1976. Infrasound from convective storms: An experimental test of electrical source mechanisms. *J. Geophys. Res*, 81, 3133

Bedard A.J. and Georges T.M. 2000. Atmospheric infrasound. *Phys. Today*, 53, 32

Bedard A. J., Bartram B. W., Keane A. N., Welsh D. C. and Nishiyama R. T. 2004a. The Infrasound Network (ISNet): Background, Design Details and Display Capability as an 88D Adjunct Tornado Detection Tool. *Proceedings of 22nd Conference on Severe Local Storms, Boston, MA, USA, 4-8 October*

Bedard A. J., Bartram B. W., Entwistle B., Golden J., Hodanish S., Jones R. M., Nishiyama R. T., Keane A. N., Mooney L., Nicholls M., Szoke E. J., Thaler E. and Welsh D. C. 2004b. Overview of the ISNet Data Set and Conclusions and Recommendations from a March 2004 Workshop to Review ISNet Data. *Proceedings of 22nd Conference on Severe Local Storms, Boston, MA, USA, 4-8 October*

Bedard A.J. 2005. Low-Frequency Atmospheric Acoustic Energy Assiciated with Vortices Produced by Thunderstorms. *Monthly Weather Review*, 133, 241

Bowman H.S. and Bedard A. J. 1971. Observations of infrasound and subsonic disturbances related to severe weather. *Geophys. J. R. Astr. Soc.*, 26, 215

Davies-Jones R.P. 1993. Helicity trends in tornado outbreaks. *Preprints of 17th Conf. on Severe Local Storms, St. Louis, MO, Amer. Meteor. Soc.*, 56-60.

Georges T.M. 1973. Infrasound from Convective Storms: Examining the Evidence. *Reviews of Geophysics and Space Physics*, 11, 571

Georges T.M. and Greene G.E. 1975. Infrasound from Convective Storms. Part IV. Is It Useful for Storm Warning?. *J. Appl. Met.*, 17, 1303

Georges T. M. 1976. Infrasound from convective storms. Part II: A critique of source candidates. NOAA Tech. Rep. ERL 380WPL 49, 59

Georges T.M. 1988 in *Instruments and Techniques for Thunderstorm Observation and Analysis*. University of Oklahoma Press (editor E. Kessler), 75

Gogoberidze G., Kahniashvili T. and Kosowsky A. 2007. Spectrum of gravitational radiation from primordial turbulence *Phys. Rev. D*, 76, 083002

Goldstein M.E. 1976. *Aeroacoustics*. McGraw Hill, New York

Goldstein M.E. 2002. A generalized acoustic analogy. *J. Fluid Mech.*, 488, 315

Hinze J.O. 1975. *Turbulence*. McGraw Hill, New York, 244

Howe M.S. 2001 in *Sound-flow interactions* (editors Y.Auregan, A.Maurel, V.Pagneux and J.F.Pinton) Springer-Verlag, Berlin, 31

Kraichnan R.H. 1964. Decay of isotropic turbulence in the Direct Interaction Approximation. *Physics of Fluids*, 7, 1163

Lemon L. R. and Doswell III C. A. 1979. Severe thunderstorm evolution and mesocyclone structure as related to tornadogenesis. *Mon. Wea. Rev.*, 107, 1184-1197

Lighthill M.J. 1952. *On Sound Generated Aerodynamically. I. General Theory*. Proc. R. Soc. London Ser. A, 211, 564

Markowski P.M., Straka J. M., Rasmussen E. N. and Blanchard D. O. 1998. Variability of storm-relative helicity during VORTEX. *Mon. Wea. Rev.*, 126, 2959-2971

Markowski P.M., Straka J.M. and Rasmussen E.N. 2002. Direct surface thermodynamic observations within the rear-flank downdrafts of nontornadic and tornadic supercells. *Mon. Weather Rev.*, 130, 16921721.

Markowski P.M., Straka J.M. and Rasmussen E.N. 2003. Tornadogenesis resulting from the transport of circulation by a downdraft. *J. Atmos. Sci.*, 60, 795823

Markowski P.M. and Richardson Y.P. 2008. Tornadogenesis: Our current understanding, forecasting considerations, and questions to guide future research. *J. Atmos. Res.*. (in press)

McCaul E.W. 1991. Buoyancy and shear characteristics of hurricane tornado environments. *Mon. Wea. Rev.*, 119, 19541978.

McCaul E.W. and Weisman M.L. 1996. Simulations of shallow supercell storms in landfalling hurricane environments. *Mon. Wea. Rev.*, 124,

DOI: 10.1002/qj

408429.

Monin A.S. and Yaglom A.M. 1975. *Statistical Fluid Mechanics*. MIT Press

Rasmussen E. N. and Blanchard D. O. 1998. A Baseline Climatology of Sounding-Derived Supercell and Tornado Forecast Parameters. *Weather and Forecasting*, 13, 4, 1148-1164

Rasmussen E. N. 2003. Refined Supercell and Tornado Forecast Parameters. *Weather and Forecasting*, 18, 3, 530-535

Rotunno R. and Klemp J. B. 1982. The influence of the shearinduced pressure gradient on thunderstorm motion. *Mon. Wea. Rev.*, 110, 136151.

Schecter D.A., Nicholls M.E., Persing J., Bedard A.J. and Pielke Sr. R.A. 2008. Infrasound emitted by tornado-like vortices: Basic theory and a numerical comparison to the acoustic radiation of a single-cell thunderstorm. *J. Atmos. Sci.*, 65, 3, 685

Stein R.F. 1967. Generation of Acoustic and Gravity Waves by Turbulence in an Isothermal Stratified Atmosphere. *Sol. Phys*. 2, 385

Szoke E.J., Bedard A.J., Thaler E. and Glancy R. 2004. A com inset data with radar data for tornadic and potentially tornac in northeast colorado. *Proceedings of 22nd Conference Local Storms, Boston, MA, USA, 4-8 October*

Thompson R. L. and Edwards R. 2000. An Overview of Envi Conditions and Forecast Implications of the 3 May 199 Outbreak. *Weather and Forecasting*, 15, 6, 682-699

Thompson R.L., Edwards R., Hart J.A., Elmore K.L. and M P.M. 2003. Close proximity soundings within supercell ments obtained from the Rapid Update Cycle. *Weather For* 12431261.

Weisman M. L. and Klemp J. B. 1982. The dependence of nu simulated convective storms on vertical wind shear and *Mon. Wea. Rev.*, 110, 504520.

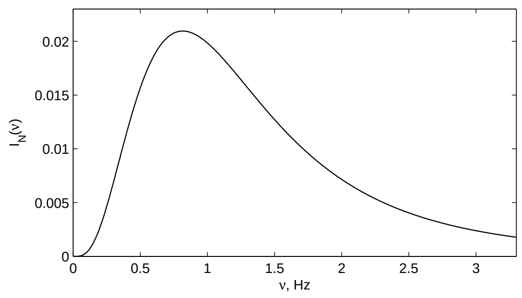

Figure 1. Normalized spectrum od acoustic radiation for the Von Karman turbulence.

Prepared using qjrms3.cls

DOI: 10.1002/qj